JOURNAL OF COMPUTATIONAL PHYSICS 46, 369–389 (1982)

Numerical Solution of an Elastic Boundary Layer Problem Using a Multiple Shooting Technique

NANCY K. NICHOLS

Department of Mathematics,
University of Reading, Whiteknights, Reading RG6 2AX Berkshire, United Kingdom

AND

ROLAND ENGLAND

IIMAS, Universidad Nacional Autónoma de México,
Apdo. Postal 20–726, Mexico 20, D.F.

Received June 15, 1981

A model is described for large axisymmetric deformations of a linearly elastic spherical shell compressed between two rigid plates. The deformation of the free region may be determined from a two-point boundary value problem, but the presence of a boundary layer makes the solution difficult by standard techniques. Solutions found by a multiple shooting method with some special features are presented here for a number of cases. Numerical evidence suggests that the onset of buckling in the contact region is controlled by a single nondimensional parameter.

1. INTRODUCTION

We describe a model for the compressive loading of a thin shell, subject to surface constraints which cause the formation of boundary layers. The mathematical model is based on a non-linear shell theory which admits large deflections and rotations and gives rise to a two-point boundary value problem. Standard numerical techniques, including simple shooting and simple finite difference procedures, were found to be unsatisfactory for obtaining solutions, due to the boundary layer formation. A modified multiple shooting method is introduced which combines the advantages of the other techniques and leads to accurate results. Numerical solutions are presented for a number of shell configurations and their implications for the buckling analysis are discussed.

In Sections 2 and 3 the physical problem and the mathematical model are described. The model derives from the analysis of Updike and Kalnins [10] and uses the non-linear shell theory of Reissner [9]. An approximate linear model is also described and the behaviour of the solutions in the boundary layer region is

0021-9991/82/060369-21$02.00/0

discussed. A special scaling of the equations is chosen to make numerical solution of the equations easier.

In Section 4 the numerical procedure for finding the solutions is presented. The method is based on the multiple shooting technique for two-point boundary value problems introduced by Osborne [7], and appears to be similar to the methods described by Kalnins [3] and Kalnins and Lestingi [4] and Wan [13] for solving these problems. A procedure of this type has also been suggested by Keller [5]. Novel features of the method described here include the automatic choice of shooting intervals and the algorithm for solving the resulting system of non-linear algebraic equations. With an appropriate formulation of the problem, a continuation method can also be implemented by the procedure to find solutions of the problem for a sequence of parameter values.

In Section 5 numerical results are presented, showing the load versus deflection behaviour of the shell, the critical points for buckling, the stress behaviour, and the yielding versus buckling points. Conclusions are given in Section 6. The results suggest that the bifurcation point at which buckling occurs depends upon a single parameter determined by the dimensions and material constants of the thin shell. The hypothesis of Updike and Kalnins [10] concerning the yielding versus buckling is also confirmed by the results.

2. Physical Problem

We consider a hollow spherical shell of isotropic material compressed between two rigid flat plates. We assume that the shell is thin, i.e., has a radius to thickness ratio $\geqslant 40$, and that the interfacial surfaces of the shell and plates slide freely. We assume further that loading is axisymmetric and that symmetry is maintained during loading, so that all displacements and stresses are independent of circumferential angle. Symmetry about the equatorial plane is also assumed.

We use the following notation: a, radius of the undeformed shell; t, thickness of the shell; E, Young's modulus of elasticity; σ, Poisson's ratio; ϕ, angle between axis of symmetry and normal of the undeformed shell; ϕ_0, value of ϕ corresponding to points at the edge of the contact region in the deformed shell; ρ_0, radius of the contact region; δ, displacement of the flat plates at equilibrium; and P, total applied pressure.

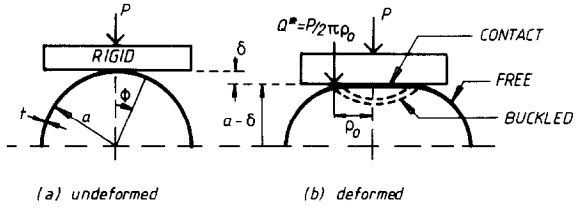

FIG. 1. (a) Undeformed, (b) deformed.

The problem is to find the equilibrium state of the shell under a given load. In the initial undeformed state (Fig. 1a) the load is concentrated at the poles. As deformation occurs, the shape of the shell is constrained by the flat plates, so that part of the shell is in contact with the plate and part of the surface remains free (Fig. 1b). The load is distributed over the area of contact between the shell and the plates, the total pressure P remaining constant. The curvature of the deformed shell is smooth and reasonably small except in the area near the edge of the contact region. Here the angle of the normal changes rapidly in order for the shell to satisfy the surface constraints. The bending moment becomes significant and the formation of a boundary layer is indicated.

As the load P increases, a bifurcation point is reached where an adjacent equilibrium state exists and the contact region may buckle inward. We assume, with some experimental justification, that the form of the first buckling mode is axisymmetric (Fig. 1b). When the load P is sufficiently large, the induced stresses in the shell may exceed the yield point and the material may become partially plastic.

For various shell configurations we wish to determine the following:

(1) load vs deflection behaviour—in particular, the relation between P and δ, the deflection of the flat plates at equilibrium, or equivalently the relation between P and ρ_0, the radius of the contact region;

(2) buckling load;

(3) maximum stresses;

(4) yielding load vs buckling load.

3. Mathematical Model

3.1 *Large Deflections and Strains—The Nonlinear Model*

The formulation of the problem is based on the analysis of Updike and Kalnins [10]. The equilibrium equations and stress–strain and strain–displacement relations are developed from Reissner's nonlinear shell theory [9]. Large deflections and rotations and large strains are admitted, but the stress–strain relationship remains linear and elastic. Bending clearly cannot be neglected, but the determination of (1) to (4) of Section 2 is essentially insensitive to shear deformation, and we may neglect transverse shear strain.

The stresses, strains, and displacements at a point on the midsurface of the deformed shell are defined in terms of the meridional angle ϕ of the original position of the point on the undeformed shell. If ϕ_0 is the value of ϕ corresponding to points on the edge of the contact region, then we can compute the stresses and deflections in the deformed shell, and also the load P, the displacement δ, and the radius ρ_0 of the contact region parametrically in terms of ϕ_0. We use the following notation (see Fig. 2): u, w, horizontal and axial displacements; β, rotation of the normal; ε_ϕ, ε_θ, meridianal and circumferential extensional strains; k_ϕ, k_θ, bending strains; N_ϕ, N_θ,

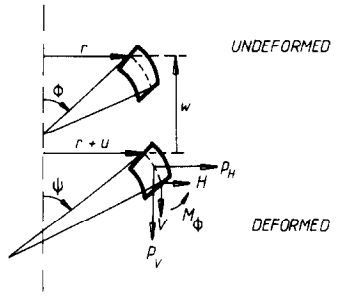

FIGURE 2.

membrane stress resultants; M_ϕ, M_θ, stress couples (or bending moments); H, V, horizontal and vertical stress resultants; p_H, p_V, loads per unit area in the horizontal and vertical directions.

The governing equations are then

(a) *Strain–displacement:*

$$\begin{aligned} \psi &= \phi - \beta \\ \varepsilon_\phi(a \sin \psi) &= dw/d\phi - a(\sin \psi - \sin \phi) \\ \varepsilon_\phi(a \cos \psi) &= du/d\phi - a(\cos \psi - \cos \phi) \\ \varepsilon_\phi &= u/(a \sin \phi) \\ k_\phi &= (1/a)\, d\beta/d\phi \\ k_\theta &= (\sin \phi - \sin \psi)/(a \sin \phi). \end{aligned} \tag{3.1a}$$

(b) *Stress–strain:*

$$\begin{aligned} N_\phi &= K(\varepsilon_\phi + \sigma\varepsilon_\theta), \qquad K = Et/(1-\sigma^2), \\ N_\theta &= K(\varepsilon_\theta + \sigma\varepsilon_\phi), \\ M_\phi &= D(k_\phi + \sigma k_\theta), \qquad D = Et^3/12(1-\sigma^2), \\ M_\theta &= D(k_\theta + \sigma k_\phi). \end{aligned} \tag{3.1b}$$

(c) *Equilibrium:*

$$\begin{aligned} dV/d\phi &= -r_1 V/\rho - v p_V \\ dH/d\phi &= -r_1 H/\rho + v N_\theta/\rho - v p_H \\ dM_\phi/d\phi &= -r_1(M_\phi - M_\theta)/\rho - v(H \sin \psi - V \cos \psi), \end{aligned} \tag{3.1c}$$

where

$$\rho = a \sin \phi + u$$

$$v = a(1 + \varepsilon_\phi)$$

$$r_1 = v \cos \psi \equiv \rho'$$

$$N_\phi = H \cos \psi + V \sin \psi.$$

In the free region, $\phi_0 \leqslant \phi \leqslant \pi/2$, the shell equations can be reduced to six ordinary differential equations for u, w, β, H, V, and M_ϕ. We normalize the variables to obtain non-dimensional quantities as

$$\hat{u} = u/a, \qquad \hat{w} = w/a, \qquad \hat{\beta} = (t/a)\beta$$

$$\hat{H} = H/Et, \qquad \hat{V} = V/Et, \qquad \hat{M}_\phi = M_\phi/Et^2.$$

This is not the standard normalization but it leads to better results for the numerical method, as we discuss later. The normalized equations are then given by

$$\begin{aligned}
\psi &= \phi - (a/t)\hat{\beta} \\
\varepsilon_\phi &= (1 - \sigma^2)(\hat{H} \cos \psi + \hat{V} \sin \psi) - \sigma \hat{u}/\sin \phi \\
d\hat{w}/d\phi &= (1 + \varepsilon_\phi) \sin \psi - \sin \phi \\
d\hat{u}/d\phi &= (1 + \varepsilon_\phi) \cos \psi - \cos \phi \\
d\hat{\beta}/d\phi &= 12(1 - \sigma^2)\hat{M}_\phi - \sigma(t/a)(\sin \phi - \sin \psi)/\sin \phi \\
d\hat{H}/d\phi &= \{(1 + \varepsilon_\phi)/(\sin \phi + \hat{u})\}\{-(1 - \sigma)\hat{H} \cos \psi + \sigma \hat{V} \sin \psi + \hat{u}/\sin \phi\} \\
d\hat{V}/d\phi &= \{(1 + \varepsilon_\phi)/(\sin \phi + \hat{u})\}\{-\hat{V} \cos \psi\} \\
d\hat{M}_\phi/d\phi &= \{(1 + \varepsilon_\phi)/(\sin \phi + \hat{u})\}\{-(1 - \sigma)\hat{M}_\phi + (t/12a)(\sin \phi \\
&\quad - \sin \psi)/\sin \phi\} \cos \psi - (1 + \varepsilon_\phi)(a/t)(\hat{H} \sin \psi - \hat{V} \cos \psi).
\end{aligned} \tag{3.2}$$

In the contact region, $0 \leqslant \phi \leqslant \phi_0$, the neglect of shear strain predicts that the pressure distribution over the contact region is zero and all the force is distributed along the edge of the contact region as a line load of magnitude $Q^* = P/2\pi\rho_0$ (see Fig. 1b). Since we are not interested in the exact pressure distribution over the contact region, but only in the relation between the total pressure P and the radius ρ_0 of the contact region, this model is sufficient. Then Eqs. (3.1a)–(3.1c) can be solved explicitly in the contact region to give

$$\begin{aligned}
\hat{w} &= \delta/a - (1 - \cos \phi) \\
\hat{\beta} &= (t/a)\phi \\
\hat{V} &\equiv 0 \\
\hat{M}_\phi &= t/(12a(1 - \sigma)) \\
\hat{H} &= f(\hat{u}),
\end{aligned} \tag{3.3}$$

where f is a known function of $\hat{u}$ and its derivative, and $\hat{u}$ satisfies the nonlinear second-order differential equation

$$\begin{aligned}&\rho(\hat{u}'' - \sin\phi + \sigma\hat{u}'/\sin\phi - \sigma\hat{u}\cos\phi/\sin^2\phi)\\&\quad + (1-\sigma)\, r_1(\hat{u} - 2\sin^2(\phi/2) - \hat{u}/\sin\phi) = 0, \qquad 0 < \phi \leqslant \phi_0,\\&\hat{u} = 0, \qquad \phi = 0.\end{aligned} \tag{3.4}$$

If we assume that the contact region is shallow so that small angle approximations are valid, i.e., $\phi \leqslant 15°$, and so that the circumferential strain is small, i.e., $1 + \varepsilon_\theta \cong 1$ in that region, then we can linearize Eq. (3.4) and solve explicitly for $\hat{u}$ in terms of an arbitrary parameter. The relation between $\hat{H}$ and $\hat{u}$ becomes simply

$$\hat{H} = f(\hat{u}) \equiv \hat{u}/((1-\sigma)\,\phi) - \phi^2/(8(1-\sigma)). \tag{3.5}$$

Equations (3.3)–(3.5) only define the solution in the contact region up to an unknown constant. If, however, we assume continuity of the variables $\hat{u}$, $\hat{\beta}$, $\hat{H}$, $\hat{M}_\phi$ between the contact region and the free region, then together with symmetry conditions at $\phi = \pi/2$, these relations give us sufficient boundary conditions to solve differential equations (3.2) in the free region. From these results we can determine the solution in the contact region uniquely. To solve the complete problem, then, we must solve differential equations (3.2) subject to the boundary conditions

$$\left.\begin{aligned}&\hat{\beta} = (t/a)\,\phi_0\\&\hat{M}_\phi = t/(12a(1-\sigma))\\&\hat{H} = \hat{u}/(1-\sigma)\,\phi_0 - \phi_0^2/8(1-\sigma)\end{aligned}\right\} \quad \text{at} \quad \phi = \phi_0,$$

$$\hat{w} = 0, \qquad \hat{\beta} = 0, \qquad \hat{H} = 0 \qquad \text{at} \quad \phi = \pi/2. \tag{3.6}$$

The vertical stress $\hat{V}$ is assumed to be discontinuous at $\phi = \phi_0$, and its limit $\hat{V}_0$, as $\phi \to \phi_0^+$ in the free region, will equal the negative of the line load Q^*. The solution of (3.2), (3.6) then gives us the values $\hat{w} = \hat{w}_0$, $\hat{u} = \hat{u}_0$, and $\hat{V} = \hat{V}_0$ at $\phi = \phi_0$ from which we can compute δ, ρ_0, and P using

$$\begin{aligned}\delta &= a(\hat{w}_0 + 1 - \cos\phi_0)\\\rho_0 &= a(\hat{u}_0 + \sin\phi_0)\\P &= -2\pi E t \hat{V}_0 \rho_0.\end{aligned} \tag{3.7}$$

We observe that Eqs. (3.2) depend on the small parameter t/a. If we examine the behaviour of the system as $t/a \to 0$, that is, as the shell becomes thinner, we find that the system reduces to the case where bending is neglected. Eliminating $\hat{M}_\phi$ from the third and sixth equations of (3.2) we derive the second-order differential equation

$$\hat{\beta}'' + \{(1-\sigma)(1+\varepsilon_\phi)/(\sin\phi + \hat{u}) + \sigma/\sin\phi\}\cos\psi\,\hat{\beta}'$$
$$+ \sigma(t/a)\sin(\psi-\phi)/\sin^2\phi - (1-\sigma)((1+\varepsilon_\phi)/(\sin\phi+\hat{u}))$$
$$\times (t/a)(\sin\phi - \sin\psi)\cos\psi/\sin\phi$$
$$= -12(1-\sigma^2)(a/t)(1+\varepsilon_\phi)(\hat{H}\sin\psi - \hat{V}\cos\psi).$$

Multiplying by t/a and formally setting $t/a = 0$, we obtain (for ϕ bounded away from zero)

$$\hat{H}\sin\psi = \hat{V}\cos\psi.$$

Substituting for ψ in the remaining equations we eliminate the effect of both $\hat{\beta}$, the rotation of the normal, and $\hat{M}_\phi$, the bending moment, and thus obtain a reduced system of order four. Evidently system (3.2) is a singular perturbation problem, and for small t/a we expect boundary layers or turning points to appear in the solution. In the physical problem the large rotations and large bending moments which occur near the edge of the contact region are responsible for the formation of boundary layers, and since the same effects occur in the solutions of the differential equations, we may reasonably assume that the mathematical model will represent the boundary layer behaviour as required.

We also observe that $\phi = 0$ is a singular point of Eqs. (3.2), and that for small values of ϕ_0 the solutions will exhibit nearly singular behaviour close to ϕ_0. This behaviour must be taken into consideration by the numerical computation procedure.

Both the boundary layer and singularity phenomena are examined in more detail in the next section with the use of an approximate linear model.

3.2 *Small Deflections and Strains—A Linear Model*

If we assume displacements and strains are small everywhere in the shell, then the limiting case of the governing equations (3.1) gives us a set of six *linear* ordinary differential equations to solve in place of (3.2). For small ϕ_0 we expect the solution of the linear equations to give us a rough approximation to the solution of the nonlinear equations. This will be useful in finding the numerical solution of the problem. The linear formulation also enables us to examine the analytical behaviour of the solutions and to test the results of the numerical procedure.

We assume that ϕ_0 is small, that the membrane strains ε_ϕ, ε_θ are small with respect to unity, and that the displacements are small. In the free region, $\phi_0 \leqslant \phi \leqslant \pi/2$, Eqs. (3.2) become

$$d\hat{w}/d\phi = (1-\sigma^2)(\hat{H}\cos\phi + \hat{V}\sin\phi)\sin\phi - \sigma\hat{u} - (a/t)\hat{\beta}\cos\phi$$
$$d\hat{u}/d\phi = (1-\sigma^2)(\hat{H}\cos\phi + \hat{V}\sin\phi)\cos\phi - \sigma\hat{u}\cot\phi + (a/t)\hat{\beta}\sin\phi$$
$$d\hat{\beta}/d\phi = 12(1-\sigma^2)\hat{M}_\phi - \sigma\hat{\beta}\cot\phi$$
$$d\hat{H}/d\phi = -(1-\sigma)\hat{H}\cot\phi + \hat{u}/\sin^2\phi + \sigma\hat{V}$$
$$d\hat{V}/d\phi = -\hat{V}\cot\phi$$
$$d\hat{M}_\phi/d\phi = -(1-\sigma)\hat{M}_\phi\cot\phi + \hat{\beta}\cot^2\phi/12 - (a/t)((\hat{H}\sin\phi - \hat{V}\cos\phi). \quad (3.8)$$

The boundary conditions are still given by (3.6). We observe that near ϕ_0 the assumptions are not strictly valid since β is not small with respect to ϕ. In absolute terms, however, both ϕ and β are small near ϕ_0, and therefore (3.8) gives a sufficiently accurate approximation to (3.2) over the free region for our purposes.

We may write Eqs. (3.8) in vector notation as

$$\mathbf{y}' = K(\phi)\,\mathbf{y}, \tag{3.9}$$

where

$$\mathbf{y}^{\mathrm{T}} = [\hat{w}, \hat{u}, \hat{\beta}, \hat{H}, \hat{V}, \hat{M}_\phi]$$

and

$$K(\phi) = \begin{bmatrix} 0 & -\sigma & -(a/t)\cos\phi & (1-\sigma^2)\sin\phi\cos\phi & (1-\sigma^2)\sin^2\phi & 0 \\ 0 & -\sigma\cot\phi & (a/t)\sin\phi & (1-\sigma^2)\cos^2\phi & (1-\sigma^2)\sin\phi\cos\phi & 0 \\ 0 & 0 & -\sigma\cot\phi & 0 & 0 & 12(1-\sigma^2) \\ 0 & 1/\sin^2\phi & 0 & -(1-\sigma)\cot\phi & \sigma & 0 \\ 0 & 0 & 0 & 0 & -\cot\phi & 0 \\ 0 & 0 & \cot^2\phi/12 & -(a/t)\sin\phi & (a/t)\cos\phi & -(1-\sigma)\cot\phi \end{bmatrix}$$

We note that the equation for $\hat{w}$ could be solved independently from the rest of the system. For numerical calculations, however, it seems more efficient to compute all the solutions simultaneously. (The same remark holds for the nonlinear model.)

The accuracy and efficiency of any numerical method for solving (3.9) depends on the conditioning of matrix $K(\phi)$ and on the range of magnitude of the nonzero coefficients. We wish to restrict the range to as small an interval as possible. For the choice of normalization, the range of magnitude is $\mathcal{O}(1) - \mathcal{O}(a/t)$. We remark that without normalizing the variable β, the range of the coefficients would be $\mathcal{O}(t/a) - \mathcal{O}(a/t)$. If none of the variables is normalized, the solutions will not be dimensionless and the equivalent Eq. (3.9) would have a matrix with coefficients in the range $\mathcal{O}(t^3/a) - \mathcal{O}(a/t^3)$. The more common normalization, in which $\hat{\beta} = \beta$ and $\hat{M}_\phi = M_\phi/Eta$, leads to a matrix with coefficients in the range $\mathcal{O}((t/a)^2) - \mathcal{O}((a/t)^2)$. The given choice of normalizing factors thus seems to lead to the best scaling of the matrix while giving dimensionless quantities.

To examine the behaviour of the solution in the region near ϕ_0, we make the assumption that angle ϕ is small, and consider the solution of Eq. (3.9) with $K(\phi)$ approximated by

$$K(\phi) \doteq \begin{bmatrix} 0 & -\sigma & -a/t & 0 & 0 & 0 \\ 0 & -\sigma/\phi & 0 & 1-\sigma^2 & 0 & 0 \\ 0 & 0 & -\sigma/\phi & 0 & 0 & 12(1-\sigma^2) \\ 0 & 1/\phi^2 & 0 & -(1-\sigma)/\phi & \sigma & 0 \\ 0 & 0 & 0 & 0 & -1/\phi & 0 \\ 0 & 0 & 1/12\phi^2 & 0 & a/t & -(1-\sigma)/\phi \end{bmatrix}.$$

Solving the fifth equation gives $\hat{V} = \hat{V}_0\phi_0/\phi$, and combining the second equation with the fourth, and third with the sixth gives

$$\hat{u}'' + \frac{1}{\phi}\hat{u}' - \frac{1}{\phi^2}\hat{u} = \frac{c_1}{\phi}$$

$$\hat{\beta}'' + \frac{1}{\phi}\hat{\beta}' - \frac{1}{\phi^2}\hat{\beta} = \frac{c_0}{\phi}$$

and

$$\hat{H} = \frac{1}{(1-\sigma^2)}\left[\hat{u}' + \frac{\sigma}{\phi}\hat{u}\right]$$

$$\hat{M}_\phi = \frac{1}{12(1-\sigma^2)}\left[\hat{\beta}' + \frac{\sigma}{\phi}\hat{\beta}\right],$$

where

$$c_0 = 12(1-\sigma^2)(a/t)\,\hat{V}_0\phi_0 \doteq -6P/\pi Et^2$$

$$c_1 = \sigma(1-\sigma^2)\,\hat{V}_0\phi_0 \doteq -\sigma P/2\pi Eta.$$

It is evident that the solutions to these equations are singular at $\phi = 0$ and therefore that, for *small* ϕ_0, the behaviour of the solutions in the region $0 < \phi_0 \leqslant \phi \ll \frac{1}{2}\pi$ is nearly singular as $\phi \to \phi_0^+$. This behaviour becomes less severe as ϕ_0 increases. The coefficients c_0, c_1 of the forcing functions, however, also increase with the total applied pressure P, and therefore, as ϕ_0 increases, the magnitudes of the solutions in the interior become larger.

For small ϕ_0 and $\phi \to \phi_0^+$, the solutions behave approximately as

$$\hat{V} \cong \hat{V}_0\phi_0/\phi$$

$$\hat{u} \cong K_1(\phi_0/\phi) + (\hat{u}_0 - K_1)(\phi/\phi_0)$$

$$\hat{\beta} \cong K_2(\phi_0/\phi) + (\hat{\beta}_0 - K_2)(\phi/\phi_0)$$

$$\hat{H} \cong K_3(1 - (\phi_0/\phi)^2) + \hat{H}_0$$

$$\hat{M}_\phi \cong K_4(1 - (\phi_0/\phi)^2) + \hat{M}_0$$

$$\hat{w} \cong K_5 \ln(\phi/\phi_0) + \hat{w}_0,$$

where $K_1 = (1+\sigma)\,\phi_0^3/16 + \frac{1}{4}c_1\phi_0$, $K_2 = \frac{1}{4}c_0\phi_0$, $K_3 = \phi_0^2/16 + c_1/4(1+\sigma)$, $K_4 = c_0/48(1+\sigma)$, $K_5 \doteq -\frac{1}{4}((a/t)\,c_0 + \sigma c_1)\,\phi_0^2$, and $\hat{\beta}_0$, $\hat{H}_0$, $\hat{M}_0$ are, respectively, the values of $\hat{\beta}$, $\hat{H}$, and $\hat{M}$ at $\phi = \phi_0$ given by (3.6). We observe that, as $\phi \to \phi_0^+$, $\hat{H}$ and $\hat{M}_\phi$ are the most badly behaved of the solution components, while $\hat{w}$ is essentially smoother than the rest.

We remark that if we formally set $t/a = 0$, the effect of both $\hat{\beta}$ and $\hat{M}_\phi$ is

eliminated from the equations, and a lower order "reduced" system is obtained (approximately equivalent to the system derived when bending is neglected). In general, the well posedness of the boundary value problem depends on the well posedness of the reduced system, provided the correct scaling of the equations has been chosen. A complete analysis of linear problem (3.8), (3.6) is possible using the theory developed by Kreiss and Nichols [6], but will not be discussed further in this paper.

3.3 *Analysis of Buckling*

To determine the minimum buckling load we assume that in the flat contact region an additional axisymmetric rotation η is superimposed on the normal rotation which is already required to satisfy the constraint imposed by the plate. The rotation of the buckled state is then

$$\beta = \phi + \eta. \tag{3.10}$$

Assuming again that the contact region is shallow, so that small angle approximations are valid, Eqs. (3.1a–c) together with (3.10) can be solved explicitly as before. Ignoring second-order terms in η, the solution for the buckled state in region $0 \leqslant \phi \leqslant \phi_0$ satisfies the original equations plus the additional second-order differential equation

$$\eta'' + \frac{\eta'}{\phi} - \left[\frac{1}{\phi^2} + \frac{k^4\phi^2}{16} - k^2\lambda^2\right]\eta = 0 \tag{3.11}$$

and boundary conditions

$$\eta(0) = 0, \qquad \eta(\phi_0) = 0. \tag{3.12}$$

Here

$$k^4 = 12(1-\sigma^2)\,a^2/t^2, \tag{3.13}$$

and λ is determined by the solution in the free region as a function of ϕ_0. (See Updike and Kalnins [10] for details.)

If λ is taken as unknown, eigenvalue problem (3.11), (3.12) can be solved to find λ^2 as a function of $k\phi_0$. The resulting curve is called the "buckling curve," and is shown in Fig. 4. (Values for the corresponding function are given in Updike and Kalnins [10].) Similarly, the curve $(\lambda^2, k\phi_0)$ can be computed directly from the solution in the free region, where λ^2 is given by

$$\lambda^2 = -k^2[\hat{H}(\phi_0) - \phi_0^2/16] \tag{3.14a}$$

or equivalently by

$$\lambda^2 = -(12(1+\sigma)\,a^2/t^2)[\hat{u}(\phi_0) - (3-\sigma)\,\phi_0^3/16]/k^2\phi_0. \tag{3.14b}$$

The bifurcation point at which buckling occurs is just the point of intersection of the two curves. To determine the critical points we solve boundary value problem (3.2), (3.6) numerically for a sequence of values of ϕ_0, compute the corresponding points on the curve $(\lambda^2, k\phi_0)$ from (3.14a), and use inverse interpolation to determine the point at which this curve crosses the "buckling curve." The numerical procedure for solving the boundary value problem is described in the next section and numerical results are given in Section 5.

4. Numerical Method

4.1 *Canonical Form of the Model*

The mathematical problem represented by the system of six differential equations (3.2) and boundary conditions (3.6) constitutes a two-point boundary value problem where the solution is required for various values of ϕ_0. The parameter ϕ_0 enters into the problem both as a boundary point, and in the boundary values at that point. To simplify the dependence upon ϕ_0, it is convenient to transform the free region to a fixed interval $[0, 1]$ in a new variable x, such that

$$\phi = (\pi/2 - \mu)\, x + \mu. \tag{4.1}$$

In terms of the new independent variable x, the values of the derivatives in (3.2) are all multiplied by $d\phi/dx = \pi/2 - \mu$, while boundary conditions (3.6) are applied at $x = 0$ or $x = 1$ as appropriate.

The problem is then in a standard form

$$d\mathbf{y}/dx = \mathbf{G}(x, \mathbf{y}(x), \boldsymbol{\mu}) \tag{4.2}$$

with boundary conditions

$$\mathbf{B}(\mathbf{y}(0), \mathbf{y}(1), \boldsymbol{\mu}) = \mathbf{0}, \tag{4.3}$$

where in this case the vector $\boldsymbol{\mu}$ has a single element $\boldsymbol{\mu} = [\mu]$, and the vector function $\mathbf{B}$ is defined by

$$\mathbf{B} \equiv \begin{bmatrix} \hat{\beta}(0) - (t/a)\,\mu \\ \hat{M}_\phi(0) - t/(12a(1-\sigma)) \\ \hat{H}(0) - \hat{u}(0)/(1-\sigma)\,\mu + \mu^2/8(1-\sigma) \\ \hat{H}(1) \\ \hat{\beta}(1) \\ \hat{w}(1) \\ \mu - \phi_0 \end{bmatrix}. \tag{4.4}$$

Here the last element is added to ensure that $x = 0$ corresponds to $\phi = \phi_0$ while allowing ϕ_0 to be varied easily. The method of continuation can then be used to solve the equations for a sequence of values of ϕ_0.

4.2 *The Multiple-Shooting Method*

The numerical solution of problem (4.2)–(4.1) is found by a "multiple-shooting" method using a general code described in detail by England [1]. The domain $[0, 1]$ is divided into subintervals, and an initial value problem with differential equation (4.2) is solved over each subinterval. The correct initial values at each "shooting" point are chosen to satisfy continuity requirements at the "matching" points at the ends of each interval, together with boundary conditions (4.3).

To describe the procedure mathematically let the vector function $\mathbf{Y}(x, z, \mathbf{W}, \boldsymbol{\mu})$ satisfy the system of differential equations

$$d\mathbf{Y}/dx = \mathbf{G}(x, \mathbf{Y}, \boldsymbol{\mu}) \tag{4.5}$$

with initial conditions

$$\mathbf{Y}(z, z, \mathbf{W}, \boldsymbol{\mu}) = \mathbf{W}. \tag{4.6}$$

The Jacobian matrices $J_W(x, z) = \partial\mathbf{Y}/\partial\mathbf{W}$ and $J_\mu(x, z) = \partial\mathbf{Y}/\partial\boldsymbol{\mu}$ then satisfy the variational equations

$$\left[\frac{dJ_W}{dt}\ \frac{dJ_\mu}{dt}\right] = \left[\frac{\partial\mathbf{G}}{\partial\mathbf{Y}}\ \frac{\partial\mathbf{G}}{\partial\boldsymbol{\mu}}\right]\begin{bmatrix} J_W & J_\mu \\ 0 & I \end{bmatrix} \tag{4.7}$$

with initial conditions

$$J_W(z, z) = I, \qquad J_\mu(z, z) = 0, \tag{4.8}$$

where I, 0 are identity and zero matrices of appropriate orders.

Given $q/2 + 1$ shooting points z_i $(i = 0, 2, \ldots, q + 1)$, and $q/2$ matching points x_i $(i = 1, 3, \ldots, q)$, such that $z_{i-1} \leqslant x_i \leqslant z_{i+1}$ and $z_{i-1} < z_{i+1}$ $(i = 1, 3, \ldots, q)$, where $z_0 = 0$, $z_{q+1} = 1$, the original boundary value problem (4.2), (4.3) reduces to a system of non-linear algebraic equations for $\mathbf{y}(z_i)$, $i = 0, 2, \ldots, q + 1$, and $\boldsymbol{\mu}$:

$$\begin{aligned} \mathbf{Y}(x_i, z_{i-1}, \mathbf{y}(z_{i-1}), \boldsymbol{\mu}) - \mathbf{Y}(x_i, z_{i+1}, \mathbf{y}(z_{i+1}), \boldsymbol{\mu}) &= \mathbf{0}, \qquad i = 1, 3, \ldots, q, \\ \mathbf{B}(\mathbf{y}(z_0), \mathbf{y}(z_{q+1}), \boldsymbol{\mu}) &= 0, \end{aligned} \tag{4.9}$$

where the values of function $\mathbf{Y}$ are determined by solving initial value problems of form (4.5), (4.6). The solution of nonlinear equations (4.9) is found using the Jacobian matrix of the system, which in this case is just the structured block matrix

$$\begin{bmatrix} J_{10} & -J_{12} & & & & K_1 \\ & J_{32} & J_{34} & & & K_3 \\ \multicolumn{6}{c}{\text{- -}} \\ & & & J_{q,q-1} & -J_{q,q+1} & K_q \\ \partial\mathbf{B}/\partial\mathbf{y}(0) & & & & \partial\mathbf{B}/\partial\mathbf{y}(1) & \partial\mathbf{B}/\partial\boldsymbol{\mu} \end{bmatrix}. \tag{4.10}$$

Here $J_{im} = J_W(x_i, z_m)$, $i = 1, 3, \ldots, q$; $m = i \pm 1$, and $K_i = J_\mu(x_i, z_{i-1}) - J_\mu(x_i, z_{i+1})$, $i = 1, 3, \ldots, q$, and both may be evaluated by solving initial value problems of the form (4.7), (4.8).

The multiple-shooting method thus consists of three principal parts: (i) selection of shooting and matching points; (ii) solution of initial value problems; (iii) solution of systems of nonlinear algebraic equations. The techniques used to implement each phase are described in the next section.

General advantages of the multiple-shooting method are mentioned in England [1]. We note that with only one "shooting" interval, the multiple-shooting technique reduces to ordinary shooting, whereas if only one step is used in the integration across each subinterval, the method reduces to a simple finite-difference method. For our problem, rapid growth of the fundamental solutions is associated with the formation of the boundary layer, and it does not seem possible to obtain a solution with less than two shooting points, thus exlcuding the ordinary shooting method. On the other hand, with the simple finite-difference procedure, a considerably larger number of nonlinear equations would need to be solved for similar accuracy and much more computer storage would be required.

4.3 *Special Features of the Multiple Shooting Method Used*

The multiple-shooting program used provides a facility for automatic selection of the shooting and matching points, in a manner which is intended both to avoid any possible ill-conditioning of the matrices J_{im} which might result from the wide span of the eigenvalues of matrix $K(\phi)$ in Eq. (3.9), and to limit the growth of integration errors within each shooting interval. The points are chosen sequentially until a final matching point x_s is found, and satisfy the following criteria along the initially estimated solution:

$$\|J_W(x_i, z_m), J_\mu(x_i, z_m)\|_\infty \simeq C, \qquad i = 1, 3, \ldots, q; \qquad \begin{cases} m = i - 1 & (i \leqslant s), \\ m = i + 1 & (i \geqslant s), \end{cases} \tag{4.11}$$

$$z_m = x_i, \qquad i = 1, 3, \ldots, q \quad (i \neq s); \qquad \begin{cases} m = i + 1 & (i < s) \\ m = i - 1 & (i > s). \end{cases} \tag{4.12}$$

Shooting is from left to right for $x < x_s$, and from right to left for $x > x_s$. First, given $z_0 = 0$, Eqs. (4.5) and (4.7) are integrated forward until the first point of the discretization where the norm in (4.11) exceeds the constant C, which has normally been taken as 10. This point is taken as x_1 and z_2. The point $x_q = z_{q-1}$ is found in a similar way by integrating backwards from $z_{q+1} = 1$. Integration then proceeds in the direction of the larger of the last two shooting intervals, the comparison being repeated after each matching point has been found, until the integrations from the two ends meet in x_s. This is a somewhat ad hoc procedure, inspired by Osborne [7], and can be sensitive to the initial estimate of the solution, as it is not convenient to modify the shooting and matching points at a later stage. Although values of C larger

than 10 may be advantageous, the procedure has generated satisfactory shooting intervals for our problem with the selected parameter values.

The method for solving initial value problems used in the program is based on a fourth-order Runge–Kutta method given by England [2] with step adjustment determined by a fifth-order local error estimate for Eq. (4.5) only (but not (4.7)).

To solve the nonlinear algebraic equations (4.9), the program uses a version of the Marquardt algorithm implemented by Reid [8] to minimize the sum of squares of the residuals. A Newton method could have been used, but the convergence of the procedure is then strongly dependent upon the initial estimate of the solution. The Marquardt-type algorithm tends to improve the global convergence properties while having the same convergence rate as the Newton method in the neighbourhood of the solution.

4.4 *Use of the Multiple Shooting Method*

For given values of the geometric and elastic parameters t/a, σ, solutions of the boundary value problem are required for various values of ϕ_0, increasing from 0, at least as far as the buckling point. For small values of ϕ_0, a good estimate of the solution is available from the linear model, and convergence to the solution of (4.9) is in any case easy and fast even from a poor estimate. For larger values of ϕ_0, however, convergence becomes slower, and it is correspondingly more difficult to provide a good initial estimate. Nevertheless, for large ϕ_0, solutions have been obtained using only crude initial estimates, as a result of the global convergence properties of the Marquardt algorithm.

It is natural, however, and quicker to use a continuation process in the parameter ϕ_0. Since results are required for various values of ϕ_0, the solution for one value may be used as the initial estimate for the next. If values of ϕ_0 are taken in increasing order, and close to one another, the initial estimates are in each case good, and rapid convergence to the solution of (4.9) is observed. As the equations are non-linear, there is also a possibility of multiple solutions. The process of continuation in ϕ_0 corresponds to the physical application of the load, and ensures convergence to the correct solution.

5. Numerical Results

Complete solutions to the thin-shell problem were obtained for a variety of physical parameters. The behaviour of the displacements and stresses was determined for values of t/a ranging from 1/40 to 1/160 and for $\sigma = 0.2$, 0.33, and 0.45. For each case, solutions were found for values of ϕ_0 ranging from $\phi_0 = 0.0436$ to $\phi_0 = 0.35$ in steps of approximately 0.02.

In Fig. 3, the load versus the deflection behaviour is shown for $\sigma = 0.33$ and various values of t/a. The bifurcation point at which buckling may occur is indicated, and it can be seen that at this point δ/t takes the same value, $\delta/t = 2.3$, in all cases, at least to a first order of accuracy.

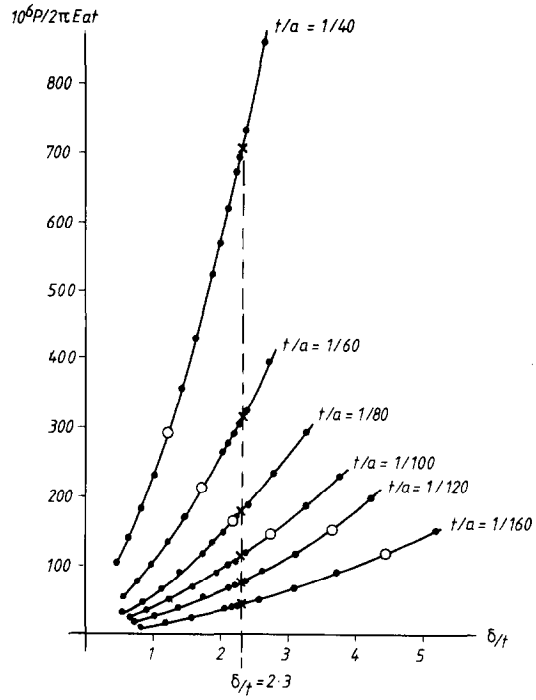

FIG. 3. ×, Buckling points; ○, approximate yield points.

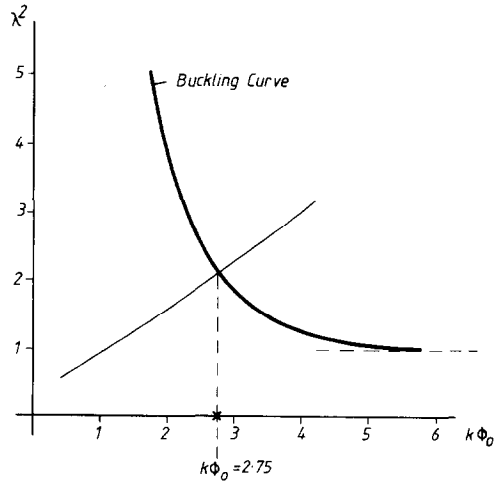

FIGURE 4.

TABLE 1

Thickness/radius t/a	ϕ_0 crit.	
	Buckling	Yielding
1/40	0.240	~0.131
1/60	0.196	~0.153
1/80	0.170	0.164
1/100	0.152	~0.175
1/120	0.139	~0.199
1/160	0.120	~0.199

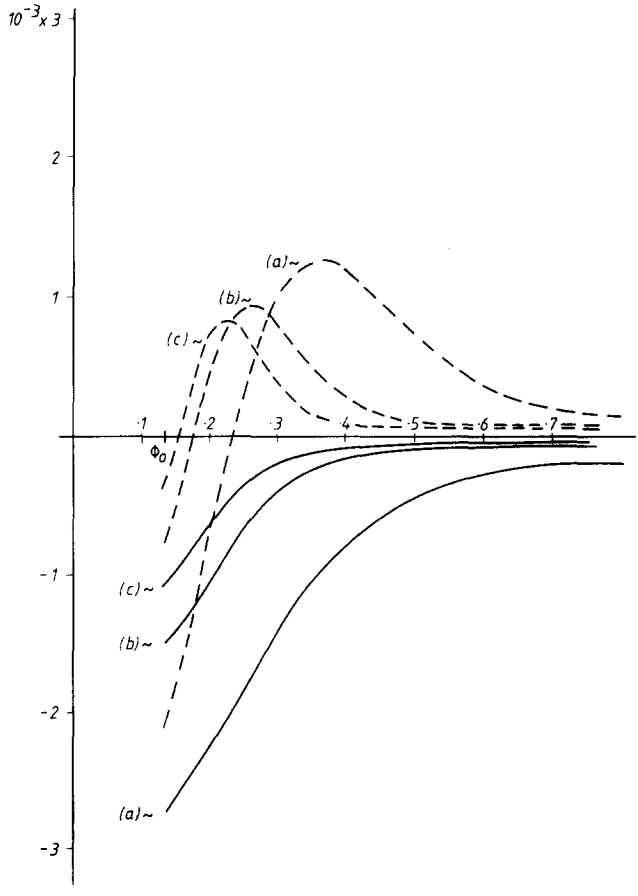

FIG. 5. $\phi_0 = 0.1312$; ---, $N_\theta/3Et$; —, $N_\phi/3Et$; (a) $t/a = 1/40$; (b) $t/a = 1/100$; (c) $t/a = 1/160$.

In Fig. 4, the "buckling curve," as defined in Section 3.3, is shown, and the curves $(\lambda^2, k\phi_0)$ computed from the solutions of the boundary value problem are plotted for $\sigma = 0.33$ and $t/a = 1/40,\ 1/80,\ 1/100,\ 1/120,\ 1/160$. The curves for the various values of t/a are virtually indistinguishable. The same curve is found in the cases $\sigma = 0.2,\ 0.45$. Near the intersection of the plotted curve with the "buckling curve," solutions were obtained for values of ϕ_0 at steps of about 0.003. In all cases the bifurcation point determined from the intersection of the curves is given to two decimal accuracy by

$$k\phi_0 = 2.75, \tag{5.1}$$

where $k = (12(1-\sigma^2)\,a^2/t^2)^{1/4}$. Hence the critical point for the buckling can be determined directly as a function of the ratio of the thickness to the radius of the shell

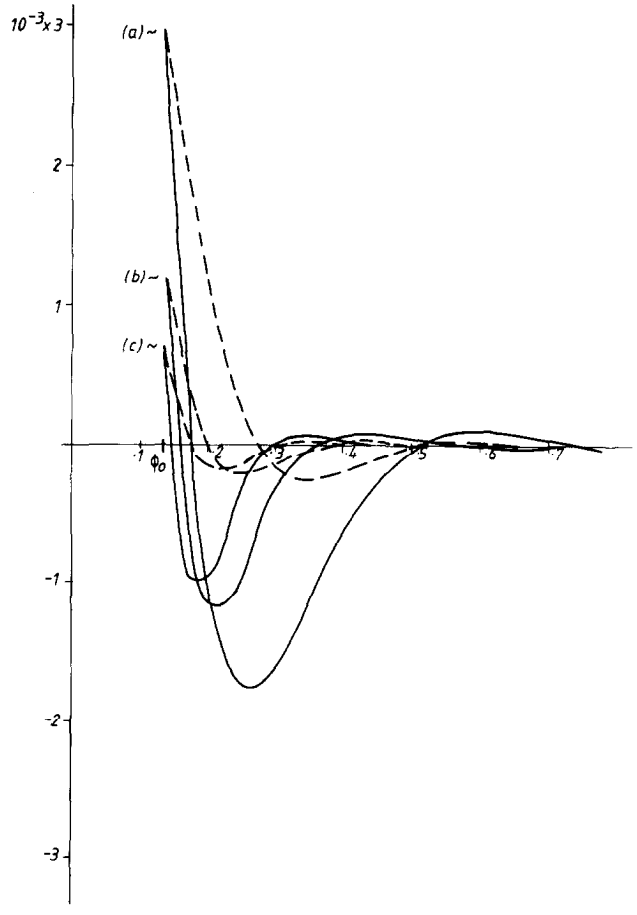

FIG. 6. $\phi_0 = 0.1312$; ---, M_θ/Et^2; —, M_ϕ/Et^2; (a) $t/a = 1/40$; (b) $t/a = 1/100$; (c) $t/a = 1/160$.

and Poisson's ratio of the material of the shell (at least for the given range of t/a). It appears also that the displacements at ϕ_0 are similarly dependent on the parameter k, and hence the value of δ/t for which buckling occurs can also be determined from k. These results do not appear to be described in the literature and no analytic proof has been found to confirm the results for all thin shells. In the case of the bending beam problem and the problem of the flat plate under compression, however, the buckling point can be shown to depend on a simple parameter determined from the dimensions and material constants of the elastic body. That such a result holds also for the thin shell does not, therefore, seem unlikely. In Table I the critical values of ϕ_0 at which buckling occurs for various t/a with $\sigma = 0.33$ are shown.

In Figs. 5–8 the distributions of the stresses and stress couples in the shell are shown for various values of ϕ_0 and t/a with $\sigma = 0.33$. We observe that for small ϕ_0,

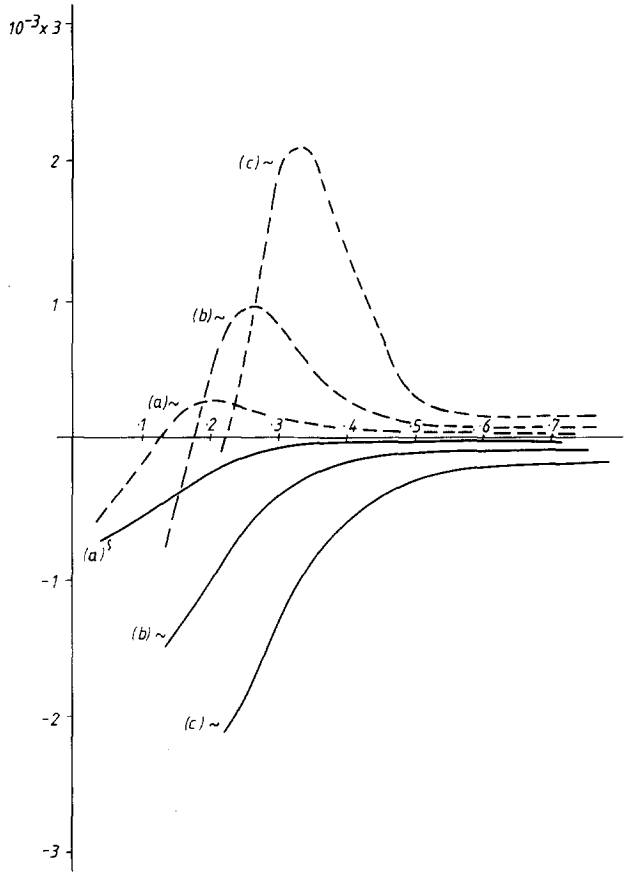

FIG. 7. $t/a = 1/100$; ---, $N_\theta/3Et$; —, $N_\phi/3Et$; (a) $\phi_0 = 0.0436$; (b) $\phi_0 = 0.1312$; (c) $\phi_0 = 0.2219$.

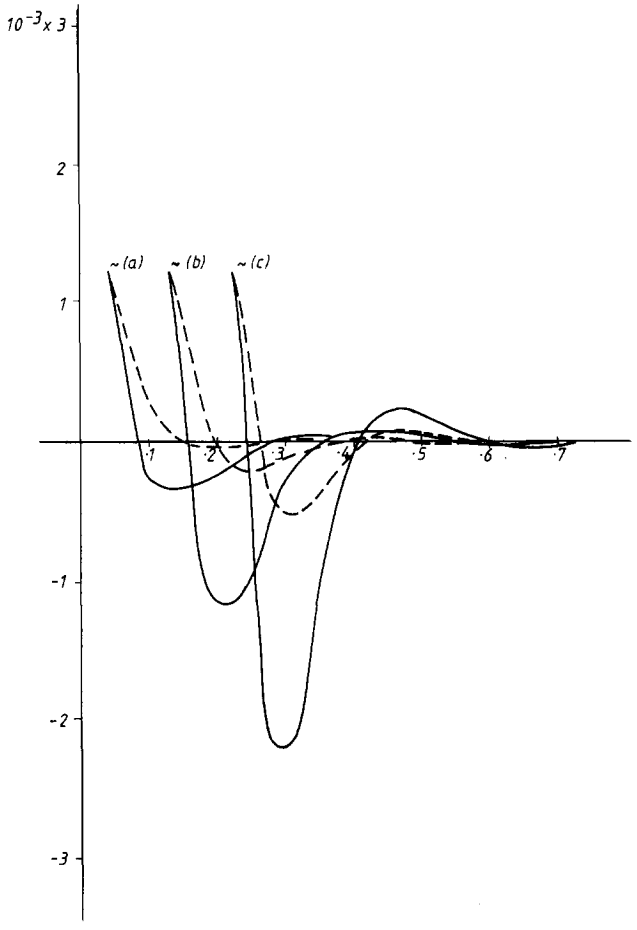

FIG. 8. $t/a = 1/100$; ---, M_θ/Et^2; —, M_ϕ/Et^2; (a) $\phi_0 = 0.0436$; (b) $\phi_0 = 0.1312$; (c) $\phi_0 = 0.2219$.

the solutions increase or decrease rapidly away from the edge of the contact region. This phenomenon is due to the nearly singular behaviour of the variable for $\phi_0 \simeq 0$ and is independent of t/a. The solutions also have large variations over a short interval in the interior adjacent to ϕ_0. This behaviour arises from the formation of the boundary layer and is worse for small t/a. We see that as t/a decreases, the width of the boundary layer decreases and the large oscillations in the solutions are pushed closer to ϕ_0. The magnitudes of the stresses decrease also with t/a and with ϕ_0, however, due to the decreased loading force P required as the shell becomes thinner, or as the compression of the shell is reduced. These results are all predicted by the analysis of the small-angle linear approximation in Section 3.2.

In all the solutions obtained, the maximum stress is caused by the meridional

bending moment and occurs in the boundary layer just outside the contact region. In most materials, yielding will occur for stresses above $E/100$, i.e., for

$$6 \max\{M_\phi\}/Et^2 \equiv 6 \max\{\hat{M}_\phi\} > 1/100. \tag{5.2}$$

Table I gives the minimum values of ϕ_0 for which the yielding condition (5.2) is satisfied for various t/a with $\sigma = 0.33$. The numerical results shown in the table confirm the hypothesis of Updike and Kalnins [10], that for large a/t (thin shells), buckling will occur before yielding, and for thicker shells the opposite will occur. Here we find that for $a/t \leqslant 80$ yielding occurs before buckling is expected, and for $a/t > 80$ buckling may be expected before yielding. In the cases $\sigma = 0.2$ and 0.45 the same result is obtained.

6. Conclusions

The mathematical model described here for the compression of a thin shell between flat plates is necessarily idealized, and a number of additional, simplifying assumptions have been made in order to obtain solutions to the problem. In particular, for the analysis of buckling, a linear approximation is taken and small-angle behaviour is assumed. The description of the buckling does not take into account any rolling or sliding of the shell surface under the plate, and friction is ignored. The pressure distribution over the plate is not considered either. More sophisticated models, incorporating some of these features have been derived by Updike and Kalnins [11, 12].

Despite the limitations of the idealized model, useful insights and conclusions can be drawn from the results. The boundary layer and singular behaviour of the solutions near the edge of the contact region with the plates is of special interest, since the membrane and rotational stresses reach maximum here. Mathematical properties of the problem related to this behaviour also cause difficulties in finding numerical solutions. We have examined the analytic behaviour of the solutions near the contact edge using small-angle approximations and have shown the singular nature of the solutions for small compression and the greater variation in the solution which occurs as the shell becomes thinner (i.e., as $t/a \to 0$).

The numerical difficulties caused by the boundary layer formation were overcome by the use of a multiple-shooting method which includes an automatic step choice and a non-linear solver with wide global convergence and quadratic local convergence. For the geometric parameters used here, the routine was able to find accurate solutions with little a priori information about the solutions. The method was adapted for continuation with respect to the loading of the shell, and a whole sequence of problems with increasing load was easily solved in one run.

The numerical results obtained suggest that in this model problem, the point at which buckling occurs is dependent on a single parameter determined by the

dimensions and material constants of the shell. These results may only hold for the range of parameters examined here. Such results, however, hold generally for other model problems, namely, the bending beam and compressed plate problems. An analytic proof for the thin-shell problem might arise from a more complete analysis of the well posedness of the model equations using singular perturbation theory. This approach will be considered in another paper.

ACKNOWLEDGMENTS

Numerical results were obtained through the computing services at AERE Harwell. The authors thank J. K. Reid of AERE for his assistance in obtaining the solutions, and also Dundee University for supporting part of this research under an NCR (National Cash Register) Fellowship.

REFERENCES

1. R. ENGLAND, UKAEA Research Group Rep. CLM–PON 3/73, Culham Laboratory, Oxford, 1976.
2. R. ENGLAND, *Comp. J.* **12** (1969), 166.
3. A. KALNINS, *J. Appl. Mech. Trans ASME* (Sept. 1964), 467.
4. A. KALNINS AND J. F. LESTINGI, *J. Appl. Mech., Trans ASME* (March 1967), 59.
5. H. B. KELLER, "Numerical Methods for Two-point Boundary Value Problems," Blaisdell, Boston, Mass., 1968.
6. H. O. KREISS AND N. K. NICHOLS, Uppsala Univ., Dept. of Computer Science Rep. 57 (Sept. 1975).
7. M. R. OSBORNE, *J. Math. Anal. Appl.* **27** (1969), 417.
8. J. K. REID, UKAEA, AERE–Harwell Rep. R7293, 1972.
9. E. REISSNER, "Proceedings, Symposium on Applied Mathematics," Vol. 3, p. 27, Amer. Math. Soc., Providence, R. I., 1950.
10. D. P. UPDIKE AND A. KALNINS, *J. Appl. Mech. Trans ASME* (Sept. 1970), 635.
11. D. P. UPDIKE AND A. KALNINS, *J. Appl. Mech. Trans ASME* (March 1972), 172.
12. D. P. UPDIKE AND A. KALNINS, *J. Appl. Mech. Trans. ASME* (Dec. 1972), 1110.
13. F. Y. M. WAN, *Mech. Today* **5** (1980), 495.